1   **SPARC: a method to genetically manipulate precise proportions of cells.**

2   Jesse Isaacman-Beck[1], Kristine C. Paik[1, 2], Carl F. R. Wienecke[1], Helen H. Yang[3],

3   Yvette E. Fisher[3], Irving E. Wang[1,4], Itzel G. Ishida[5], Gaby Maimon[5], Rachel I. Wilson[3],

4   Thomas R. Clandinin[1*]

5

6   **AFFILIATIONS**

7   [1]Department of Neurobiology, Stanford University, Stanford, CA 94305

8   [2]Present address: Department of Medicine, Weill Cornell Medical College, New York,

9   NY 10065

10   [3]Department of Neurobiology and Howard Hughes Medical Institute, Harvard Medical

11   School, Boston, MA 02115

12   [4]Present address: Freenome, South San Francisco, CA 94080

13   [5]Laboratory of Integrative Brain Function and Howard Hughes Medical Institute, The

14   Rockefeller University, New York, NY 10065

15   [*]Correspondence: trc@stanford.edu

16

17   **Abstract**

18   Many experimental approaches rely on controlling gene expression in select subsets of

19   cells within an individual animal. However, reproducibly targeting transgene expression

20   to specific fractions of a genetically-defined cell-type is challenging. We developed

21   Sparse Predictive Activity through Recombinase Competition (SPARC), a generalizable

22   toolkit that can express any effector in precise proportions of post-mitotic cells in

23   *Drosophila*. Using this approach, we demonstrate targeted expression of many

24   effectors and apply these tools to calcium imaging of individual neurons and optogenetic

25   manipulation of sparse cell populations *in vivo*.

26   **Main Text**

27   Genetic labeling and manipulation of small groups of cells in somatic mosaic

28   animals have provided significant insights into many aspects of biology and have been

29   particularly impactful in studies of the nervous system. Indeed, measurement and

30   manipulation of genetically defined cell types has become central to neural circuit

31   dissection in many systems[1]. Especially powerful are paradigms in which one measures

32   the phenotypes of stochastically selected individual cells within otherwise

33   unmanipulated populations. However, few methods exist for selectively manipulating a

34   desired fraction of cells of the same genetically-defined type. In rodents, sequential

35   recombinase-mediated switches can label subpopulations of neurons, but require labor-

36   intensive titration of viruses[2]. In *Drosophila*, GAL4 and split GAL4 lines enable targeting

37   of single cell types[3], but selective manipulation of subsets of neurons of the same type

38   remains challenging. For example, effector expression can be restricted by limiting the

39   spatial and/or temporal expression of a recombinase, but this necessitates user-

40   dependent heat shock or chemical induction, and in some cases, cannot be used in

41   post-mitotic cells[4-6]. Therefore, a routine all-genetic method of expressing effectors in

42   defined fractions of post-mitotic cells of the same type would provide a powerful means

43   of dissecting cellular and genetic functions.

44   To address this need, we developed SPARC, a toolkit to express any effector in

45   precise proportions of post-mitotic cells labelled by the GAL4-UAS system (Fig. 1A, S1,

46   S2)[7]. The core of this toolkit is a set of bistable UAS-driven constructs that can be

47   switched on or off in different relative proportions of cells, depending on their

48   sequences. We designed each UAS-driven construct, so that PhiC31 recombinase[8]

49   could irreversibly recombine one of two competing *attP* target sequences with one *attB*

50   target sequence. The reaction mediated by the first *attP* would remove a stop cassette

51   to enable effector expression in cells expressing Gal4, while the reaction using the

52   second *attP* would leave this stop intact and prevent expression (Fig. S1). Truncating

53   canonical *attP* sequences diminishes the efficacy of recombination *in vitro*[9]. Based on

54   this, we reasoned that truncating the first *attP* relative to the second would shift the

55   equilibrium to favor retention of the stop cassette and result in sparser effector

56   expression *in vivo*.

57   To test this concept, we generated plasmids and transgenic flies bearing SPARC

58   constructs expressing the calcium indicator GCaMP6f[10] and including one of three

59   different *attP* variants at the first position (canonical: attP60; truncated: attp38 or

60   attp34)[9]. We also generated transgenic flies that express PhiC31 recombinase in all

61   post-mitotic neurons under the control of the synaptobrevin promoter[3]. We then drove

62   expression of each SPARC construct in one of the largest genetically-defined

63   populations of neurons in the *Drosophila* optic lobe, T4 and T5 cells[11], in animals that

64   express PhiC31 pan-neuronally. Across SPARC-GCaMP6f variants, we observed

65   progressively fewer labeled neurons (Fig. 1C-E). SPARC-*attP60*-GCaMP6f labeled

66   many overlapping neurons, SPARC-*attP38*-GCaMP6f labeled an intermediate number

67   of neurons and SPARC-*attP34*-GCaMP6f labeled individual neurons whose dendrites

68   could be visualized (Fig 1E inset). We therefore named these variants SPARC-D

69   (Dense), SPARC-I (Intermediate), and SPARC-S (Sparse). To determine the

70   percentage of these neurons labeled by each SPARC module, we expressed

71   myristoylated-tdTomato (myr-tdT) in all T4 and T5 neurons in parallel with SPARC-

72   GCaMP6f and counted singly and doubly labeled T4 and T5 cell bodies (Fig. 1F and

73   S3). For SPARC-D-GCaMP6f we observed effector expression in ~45% of T4 and T5

74   neurons. In comparison, SPARC-I-GCaMP6f labeled ~12% of T4 and T5 neurons, while

75   SPARC-S-GCaMP6f labeled only ~4% of these neurons. We observed similar results in

76   Kenyon cells, Lobula-Columnar neurons, and several columnar neurons in the optic

77   lobe (Fig. S4 and data not shown). These data demonstrate that the SPARC module

78   can reproducibly determine the fraction of cells that express effector over a more than

79   10-fold range across cells and animals. As SPARC-S can readily label T4, T5 and

80   Kenyon cells, very common cell types in the fly brain, these studies argue that one of

81   the three SPARC modules should allow targeting of individual cells of any cell type of

82   interest.

83   To generalize this technique, we next made SPARC-LexA::p65 transgenes.

84   LexA::p65 is a transcription factor that drives expression of transgenes under the control

85   of the lexAop promoter[12]; this system is orthogonal to the UAS-GAL4 expression

86   system. We expressed SPARC-LexA::p65 in Mi1 neurons of the *Drosophila* optic lobe

87   (Fig 1B), and found that in the absence of PhiC31 recombinase, SPARC-LexA::p65

88   labels 100% of these neurons with lexAop-myr-tdT (Fig. 1G-G''). This result suggested

89   that the widely-used stop cassette[13] that we used in the initial SPARC design might

90   permit a low level of read-through that can be detected by sensitive outputs like

91   LexA::p65 (or mCD8::GFP, data not shown).

92   To avoid this read-through, we generated SPARC2, in which we incorporated two

93   self-cleaving ribozymes from the Hepatitis Delta Virus (HDV) into the SPARC module

94   (Fig. 1A). We reasoned that these self-cleaving ribozymes should truncate any read-

95   through transcript prior to translation[14,15]. We first examined SPARC2-LexA::p65

96   transgenes in Mi1 neurons in the absence of PhiC31 and observed a 10,000-fold

97   decrease in read-through (~0.01% of Mi1 labeled with lexAop-myr-tdT, Fig. 1H-H'').

98   Importantly, the D, I, and S variants of SPARC2-LexA::p65 behaved similarly to

99   SPARC-GCaMP6f transgenes (Fig. 1I–K''). Also quantitative measurement of SPARC2-

100   mCD8::GFP in Mi1 cells showed the same three levels of expression(Figure S4I-L).

101   Thus, HDV ribozymes effectively eliminate read-through and enable SPARC2

102   transgenes to express both direct and amplifying effectors in three different proportions

103   of cells.

104   Next, to investigate the functional utility of SPARC, we first used SPARC-S-

105   GCaMP6f to image calcium (Ca^{2+}) response in the dendrites of individual T5 neurons.

106   These neurons preferentially respond to visual motion in one direction, a direction

107   selectivity that is first observed in their dendrites[16]. Previous attempts to image from

108   individual T5 cells relied on laborious FlpOut approaches that required titrated and

109   temporally precise heat shocks of *Drosophila* larvae to restrict effector expression to a

110   subset of cells[16-18]. In contrast, the SPARC method consistently labeled fewer T5

111   neurons, and labeled them more sparsely, than the sparsest FlpOut labeling using brief

112   and developmentally late heat-shock (Fig. 1E, 2A,B). More importantly, when we

113   imaged visually-evoked Ca^{2+} responses in regions of interest (ROIs) representing T5

114   dendrites, we observed that the fluorescent signals from SPARC-labeled ROIs were

115   significantly more direction selective than those from FlpOut-labeled ROIs (DSI; Fig. 2C-

116   E). This result reflects the fact that SPARC labeling was sparser than the sparsest

117   FlpOut labeling we could achieve. As a consequence, SPARC ROIs more nearly

118   captured signals from single cells, while FlpOut ROIs likely included signals from

119   multiple labeled cells with different directional preferences (see supplemental methods).

120   Thus, both anatomical and functional evidence suggests that SPARC better isolates

121   single T5 dendrites more easily and more consistently than standard FlpOut

122   approaches.

123   Then, to determine if we could use this approach to manipulate the activity of

124   neuronal subpopulations, we generated SPARC2-CsChrimson::tdTomato[19] transgenic

125   flies. We expressed this construct in Ring (R) neurons, GABAergic neurons that send

126   sensory input to the central complex[20]. R neurons are divided into types based on

127   morphology[21], here we focused on the R2 type. We expressed SPARC2-D-

128   CsChrimson::tdTomato in a subset of R2 neurons (Figures 2F-H"). We observed that

129   tdTomato$^+$ R2 neurons were depolarized by light, while tdTomato$^-$ R2 neurons were not

130   depolarized (Figure 2I, J). Indeed, tdTomato$^-$ R2 neurons were slightly hyperpolarized

131   by light (Figure 2I, J), implying that these R2 neurons were postsynaptic to other R2

132   neurons that express CsChrimson. Thus, the SPARC system enables optogenetic

133   activation of sparse cell populations within a single cell type, allowing us to discover

134   evidence for mutual inhibitory interactions within a cell type. Although it was already

135   known that some R neuron types inhibit other R types[20], it was not previously known

136   that there is mutual inhibition between R neurons of the same type.

137   The SPARC and SPARC2 toolkit includes direct effector transgenes that can be

138   used to label cells (mCD8::GFP), to observe changes in intracellular calcium

139   concentration (GCaMP6f, jGCaMP7f) and membrane potential (ASAP2f), as well as to

140   optogenetically modulate neuronal activity (CsChrimson). In addition, the availability of

141   the indirect effector transgene SPARC2-LexA::p65 opens the possibility of sparsely

142   expressing a large range of additional existing effectors under the control of lexAop

143   (Figure S5). To provide the flexibility to target both neuronal and non-neuronal cells, we

144   also generated transgenic animals that express PhiC31 pan-neuronally (nSyb-PhiC31),

145   ubiquitously (tub-PhiC31) and in any cell type labeled by GAL4 (UAS-PhiC31). Thus, by

146   simply generating flies with the appropriate combination of transgenes (Fig. S6), one

147   can perform a diverse array of experiments on single cells or precise proportions of cells

148   of a given genetically defined type. Moreover, each element of this toolkit is modular,

149   allowing users to easily incorporate any current or future genetically encoded effector

150   (Fig. S3). In the context of the nervous system, SPARC, SPARC2 and future variations

151   will allow convenient and unparalleled access to define the heterogeneity of single

152   neuron contributions to neural circuit processing. In non-neuronal cells, SPARC will

153   enable wide-ranging studies that exploit mosaic analysis to investigate the cell biology

154   and physiology of post-mitotic cells. Finally, as PhiC31 functions in both the mouse and

155   fish[22,23], we anticipate that this strategy will be widely generalizable to other model

156   systems.

157

171

172   **Author contributions:** J.I-B., H.H.Y, I.E.W. and T.R.C conceived the study. J.I-B,

173   C.F.R.W., H.H.Y., and Y.E.F. designed and performed the experiments under the

174   supervision of T.R.C. and R.I.W. J.I-B., K.C.P., H.H.Y., Y.E.F., and I.G.I generated,

175   maintained, and/or validated transgenic fly stocks under the supervision of T.R.C,

176   R.I.W., and G.M. J.I-B., C.F.R.W., H.H.Y., Y.E.F. and K.C.P. analyzed the data. J.I-B.

177   and T.R.C. prepared the manuscript with contributions from C.F.R.W., H.H.Y., and

178   Y.E.F.

179

180   **Competing Interests statement:** The authors declare no competing financial interests.

181

182   **Methods:** Attached as Supplemental Methods.

References:

1. Luo, L., Callaway, E. M. & Svoboda, K. Genetic Dissection of Neural Circuits: A Decade of Progress. *Neuron* **98,** 256–281 (2018).

2. Lin, R. *et al.* Cell-type-specific and projection-specific brain- wide reconstruction of single neurons. *Nat. Methods* 1–9 (2018). doi:10.1038/s41592-018-0184-y

3. Jenett, A. *et al.* A GAL4-driver line resource for Drosophila neurobiology. *CellReports* **2,** 991–1001 (2012).

4. Lee, T. & Luo, L. Mosaic analysis with a repressible cell marker for studies of gene function in neuronal morphogenesis. *Neuron* **22,** 451–461 (1999).

5. Del-Valle-Rodriguez, A., Didiano, D. & Desplan, C. Power tools for gene expression and clonal analysis in Drosophila. *Nat. Methods* **9,** 47–55 (2011).

6. Sethi, S. & Wang, J. W. A versatile genetic tool for post-translational control of gene expression inDrosophila melanogaster. *eLife* **6,** e04577 (2017).

7. Brand, A. H. & Perrimon, N. Targeted gene expression as a means of altering cell fates and generating dominant phenotypes. *Development* **118,** 401–415 (1993).

8. Groth, A. C., Olivares, E. C., Thyagarajan, B. & Calos, M. P. A phage integrase directs efficient site-specific integration in human cells. *Proc. Natl. Acad. Sci. U.S.A.* **97,** 5995–6000 (2000).

9. Groth, A. C., Olivares, E. C., Thyagarajan, B. & Calos, M. P. A phage integrase directs efficient site-specific integration in human cells. *Proc. Natl. Acad. Sci. U.S.A.* **97,** 5995–6000 (2000).

10. Chen, T.-W. *et al.* Ultrasensitive fluorescent proteins for imaging neuronal activity. *Nature* **499,** 295–300 (2013).

206   11.   Pinto-Teixeira, F. *et al.* Development of Concurrent Retinotopic Maps in the Fly

207   Motion Detection Circuit. *Cell* 1–26 (2018). doi:10.1016/j.cell.2018.02.053

208   12.   Lai, S.-L. & Lee, T. Genetic mosaic with dual binary transcriptional systems in

209   Drosophila. *Nat Neurosci* **9,** 703–709 (2006).

210   13.   Pfeiffer, B. D. *et al.* Refinement of Tools for Targeted Gene Expression in

211   Drosophila. *Genetics* **186,** 735–755 (2010).

212   14.   Perrotta, A. T. & Been, M. D. A pseudoknot-like structure required for efficient

213   self-cleavage of hepatitis delta virus RNA. *Nature* **350,** 434–436 (1991).

214   15.   Wernet, M. F., Klovstad, M. & Clandinin, T. R. A Drosophila toolkit for the

215   visualization and quantification of viral replication launched from transgenic

216   genomes. *PLoS ONE* **9,** e112092 (2014).

217   16.   Fisher, Y. E., Silies, M. & Clandinin, T. R. Orientation Selectivity Sharpens Motion

218   Detection in Drosophila. *Neuron* **88,** 390–402 (2015).

219   17.   Leong, J. C. S., Esch, J. J., Poole, B., Ganguli, S. & Clandinin, T. R. Direction

220   Selectivity in Drosophila Emerges from Preferred-Direction Enhancement and

221   Null-Direction Suppression. *Journal of Neuroscience* **36,** 8078–8092 (2016).

222   18.   Wienecke, C. F. R., Leong, J. C. S. & Clandinin, T. R. Linear Summation

223   Underlies Direction Selectivity in Drosophila. *Neuron* 1–14 (2018).

224   doi:10.1016/j.neuron.2018.07.005

225   19.   Klapoetke, N. C. *et al.* Independent optical excitation of distinct neural

226   populations. *Nat. Methods* **11,** 338–346 (2014).

227   20.   Xie, X. *et al.* The laminar organization of the Drosophila ellipsoid body is

228   semaphorin-dependent and prevents the formation of ectopic synaptic

229   connections. *eLife* **6,** e04577 (2017).

230   21.   Omoto, J. J. *et al.* Neuronal Constituents and Putative Interactions Within the

231   Drosophila Ellipsoid Body Neuropil. *Front. Neural Circuits* **12,** 103 (2018).

232   22.   Mosimann, C. *et al.* Site-directed zebrafish transgenesis into single landing sites

233   with the phiC31 integrase system. *Dev. Dyn.* **242,** 949–963 (2013).

234   23.   Olivares, E. C. *et al.* Site-specific genomic integration produces therapeutic Factor

235   IX levels in mice. *Nature Biotechnology* **20,** 1124–1128 (2002).

236   24.   Wystrach, A., Dewar, A. D. M. & Graham, P. Insect Vision: Emergence of Pattern

237   Recognition from Coarse Encoding. *Current Biology* **24,** R78–R80 (2014).

238

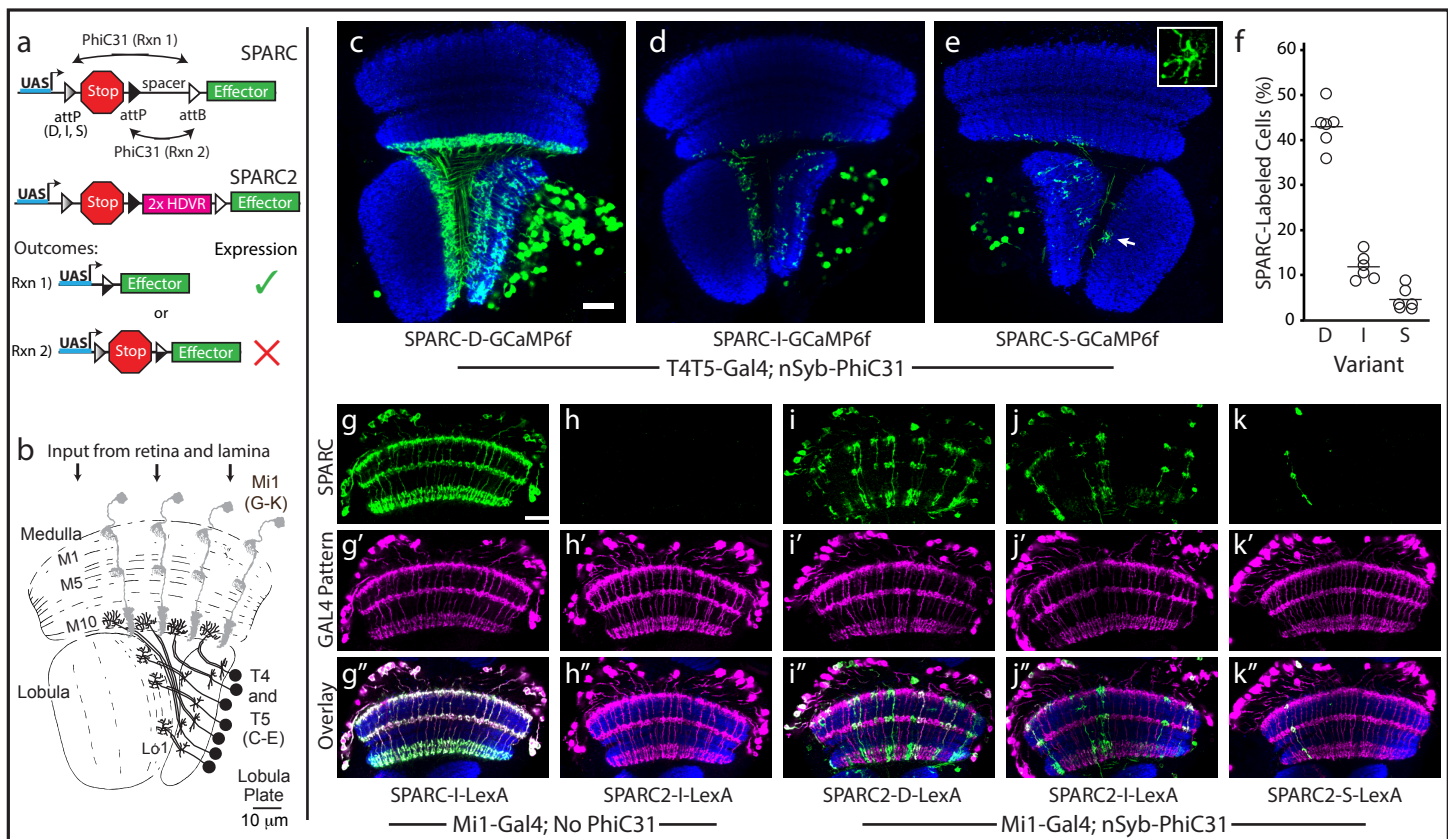239   **Main Figures and Figure Legends:** Attached Below.

Figure 1: SPARC and SPARC2 enable predictive expression of effectors at three levels. (a) Schematic of SPARC and SPARC2 modules. PhiC31 recombines one of two competing attP target sequences with one attB target sequence. Truncating the first attP progressively favors retention of the stop cassette, preventing expression (Dense-60bp, canonical sequence; Intermediate - 38bp; Sparse – 34bp). SPARC2 incorporates a 2X Hepatitis Delta Virus Ribozyme (HDVR) sequence to prevent read-through in the absence of PhiC31. **(b)** Schematic of the *Drosophila* optic lobe highlighting T4, T5 and Mi1. **(c-e)** GCaMP6f expression (green) in T4 and T5 neurons counterstained with anti-Bruchpilot (blue). (c) SPARC-D-GCaMP6f (d) SPARC-I-GCaMP6f (e) SPARC-S-GCaMP6f, arrow points to dendrite shown in inset **(f)** Percentage of T4 and T5 neurons labeled by different SPARC modules (see Fig. S3). N = 6 optic lobes and > 400 cell bodies/genotype. **(g-k)** LexA::p65-driven expression of lexAop-myr-tDT (green, g-k), in Mi1 neurons (magenta, g'-k') counterstained with anti-Bruchpilot (blue, overlay, g"-k"). (g) SPARC-I-LexA::p65 no PhiC31. LexA::p65 is expressed in all Mi1 neurons in the absence of PhiC31 in these animals. (h) SPARC2-I-LexA::p65 no PhiC31. LexA::p65 is not expressed in Mi1 neurons in the absence of PhiC31, consistent with an absence of read-through. (i) SPARC2-D-LexA::p65. (j) SPARC2-I-LexA::p65 (k) SPARC2-S-LexA::p65. Scale bars, 10 µm; N > 10 optic lobes per condition.

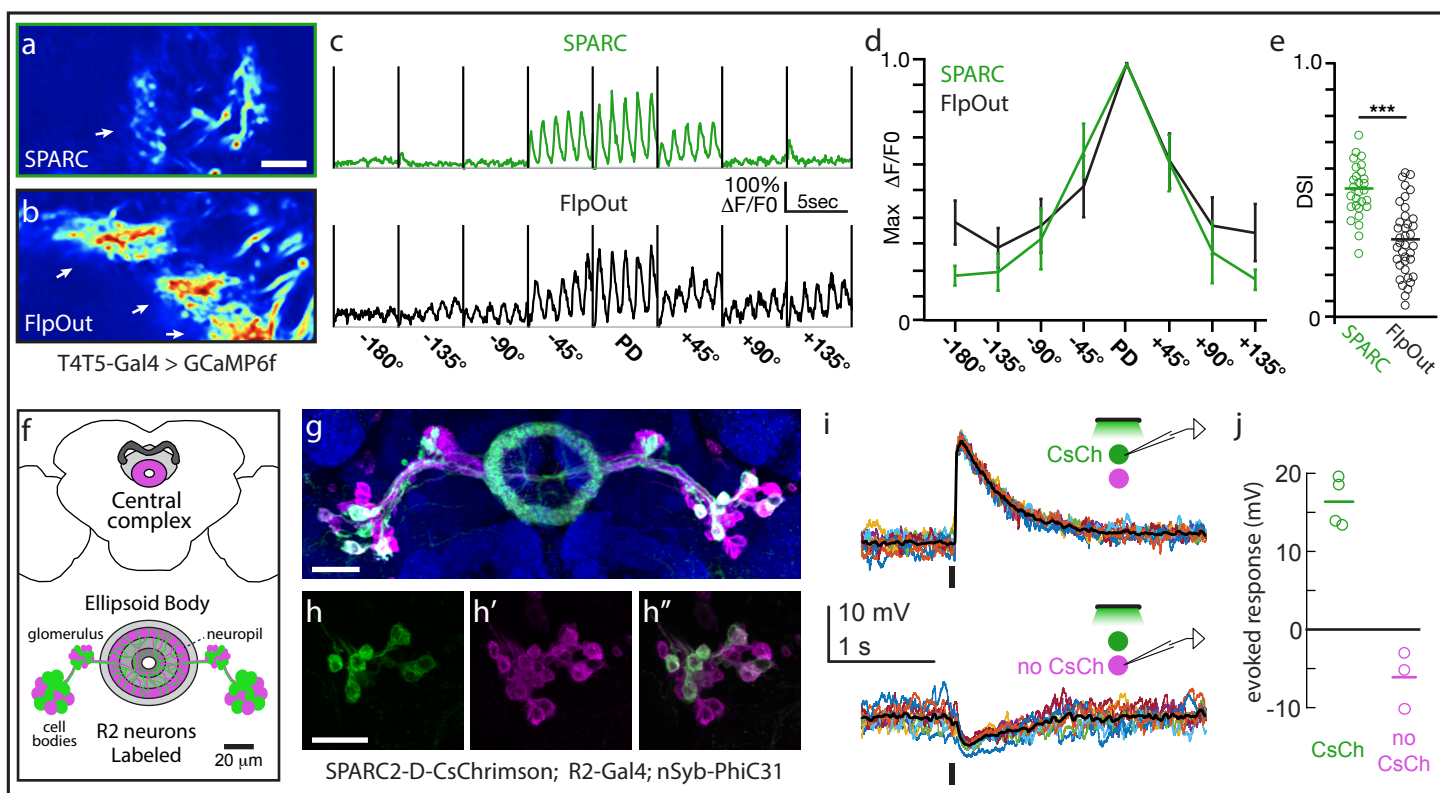Isaacman-Beck et al., 2019. Figure 1.

Figure 2: SPARC and SPARC2 enable calcium imaging of single neurons and optogenetic stimulation of sparse cell populations. (a, b) Normalized averaged fluorescence intensity of GCaMP6f in T5 dendrites sparsely labeled using (a) SPARC-S-GCaMP6f or (b) FlpOut-GCaMP6f. Arrows point to dendrites. **(c-d)** GCaMP6f fluorescence responses (ΔF/F0) of T5 dendritic ROIs to sinusoidal gratings moving in one of eight different directions. PD denotes the preferred direction of each cell with the angular deviation from PD in degrees (c) Averaged responses of a representative ROI labeled using SPARC-S-GCaMP6f (green) or FlpOut-GCaMP6f (black). (d) Normalized tuning curves averaged across all T5 dendritic ROIs labeled by SPARC-S-GCaMP6f (green) or FlpOut-GCaMP6f (black) **(e)** Direction selectivity indices (DSI) for each T5 dendritic ROI labeled by SPARC-S-GCaMP6f or FlpOut-GCaMP6f, n = 8 flies and 37 units per condition; *** $p < 0.001$. **(f)** Schematic of Central Complex and Ellipsoid Body depicting SPARC2-labeled R2 Ring neurons (adapted from24). **(g)** SPARC2-D-CsChrimson::tdTomato-3.1 expression (tdTomato; green) in R2 Ring neurons (mCD8::GFP; magenta) counterstained with anti-Bruchpilot (blue). **(h-h")** Closeup of cell bodies in (g) showing (h) CsChrimson expression in (h') R2 cells. (h") Overlay. **(I)** Current clamp recordings of single tdTomato+ (top) and tdTomato- (bottom) R2 neurons. Stimulus is a 50 ms pulse of green light; 10 trials each (colored lines), mean response (black line). **(j)** Average evoked response (open circles) and mean population response (line) of R2 neurons, both tdTomato+ (green, N =4) and tdTomato- (magenta, N = 3). Scale bars: 10 µm (a,b), 20 µm (g, h).

Isaacman-Beck et al., 2019. Figure 2.